Stromal markers of activated tumor associated fibroblasts predict poor survival and are associated with necrosis in non-small cell lung cancer

Jordi Alcaraz[a,b,c,d,*], Josep Lluís Carrasco[e], Laura Millares[b,c,f], Iuliana-Cristiana Luis[a], Francisco J. Fernández-Porras[a], Anabel Martínez-Romero[b,g], Natalia Diaz-Valdivia[a], Julio Sánchez De Cos[b,c,h], Ramon Rami-Porta[b,c,i], Luis Seijo[c,j], Josep Ramírez[k], María José Pajares[c,l], Noemí Reguart[m], Esther Barreiro[b,c,g], Eduard Monsó[b,c,f,n]

[a] Unit of Biophysics and Bioengineering, Department of Biomedicine, School of Medicine and Health Sciences, Universitat de Barcelona, Barcelona, Spain
[b] CIBER de Enfermedades Respiratorias — CIBERES, Instituto de Salud Carlos III, Madrid, Spain
[c] Grupo Colaborativo en Cáncer de Pulmón CIBERES-CIBERONC-SEPAR-Plataforma Biobanco Pulmonar, Spain
[d] Institute for Bioengineering of Catalonia (IBEC), The Barcelona Institute for Science and Technology (BIST), Barcelona, Spain
[e] Unit of Biostatistics, Department of Basic Clinical Practice, School of Medicine and Health Sciences, Universitat de Barcelona, Barcelona, Spain
[f] Respiratory Medicine, Hospital Universitari Parc Taulí, Sabadell, Spain
[g] Muscle Wasting and Cachexia in Chronic Respiratory Diseases and Lung Cancer, IMIM-Hospital del Mar, CEXS, UPF, PRBB, Barcelona, Spain
[h] Hospital San Pedro de Alcántara, Cáceres, Spain
[i] Hospital Universitari Mutua Terrassa, Terrassa, Spain
[j] Fundación Jímenez Díaz, Madrid, Spain
[k] Anatomopathology Department, Hospital Clínic de Barcelona, Barcelona, Spain
[l] Program in Solid Tumors and Biomarkers, Center for Applied Medical Research (CIMA) and CIBERONC, Pamplona, Spain
[m] Medical Oncology Department, Hospital Clínic de Barcelona, IDIBAPS, Barcelona, Spain
[n] Department of Medicine, Universitat Autònoma de Barcelona (UAB), Barcelona, Spain

ARTICLE INFO

ABSTRACT

Objectives: Tumor associated fibroblasts (TAFs) are essential contributors of the progression of non-small cell lung cancer (NSCLC). Most lung TAFs exhibit an activated phenotype characterized by the expression of α-SMA and fibrillar collagens. However, the prognostic value of these activation markers in NSCLC remains unclear.
Material and Methods: We conducted a quantitative image analysis of α-SMA immunostaining and picrosirius red staining of fibrillar collagens imaged by bright-field and polarized microscopy, respectively, using tissue microarrays with samples from 220 surgical patients, which elicited a percentage of positive staining area for each marker and patient.
Results: Kaplan-Meier curves showed that all TAF activation markers were significantly associated with poor survival, and their prognostic value was independent of TNM staging as revealed by multivariate analysis, which elicited an adjusted increased risk of death after 3 years of 129% and 94% for fibrillar collagens imaged with bright-field ($p = 0.004$) and polarized light ($p = 0.003$), respectively, and of 89% for α-SMA ($p = 0.009$). We also found a significant association between all TAF activation markers and tumor necrosis, which is often indicative of hypoxia, supporting a pathologic link between tumor desmoplasia and necrosis/hypoxia.
Conclusions: Our findings identify patients with large histologic coverage of fibrillar collagens and α-SMA + TAFs to be at higher risk of recurrence and death, supporting that they could be considered for adjuvant therapy.

1. Introduction

Lung cancer is the leading cause of cancer-related death in both men and women worldwide, with an overall 5 year survival rate of 18% [1,2]. This leading position is partly associated with the fact that most lung cancer patients remain undiagnosed until the disease is symptomatic and has reached an advanced stage [3]. Surgically-treated patients tend to exhibit better prognosis, particularly when diagnosed at early stages, but still have a suboptimal potential cure of only ˜30-50% [1].

Histologically, non-small cell lung cancer (NSCLC) is diagnosed in up to 90% of lung cancer patients, and adenocarcinoma (ADC) and squamous cell carcinoma (SCC) are the major subtypes [1]. Because these lung cancer subtypes are epithelial in origin, most previous studies have focused on the pathologic features of lung carcinoma cells. However, it is increasingly acknowledged the prominent role of the stiff desmoplastic tumor stroma that surrounds carcinoma cells in the progression of lung cancer and other solid tumors [4]. This desmoplastic stroma is rich in activated fibroblasts (referred to as cancer- or tumor-associated fibroblasts (TAFs)), infiltrated immune cells and other less frequent cell types, in the background of an abundant deposition of fibrillar collagens and other fibrotic extracellular matrix components [4,5]. Of note, TAFs are largely responsible for the aberrant stromal deposition of fibrillar collagens within the tumor stroma [6], and are receiving increasing interest as a therapeutic target [7], as illustrated by the recent approval of the antiangiogenic and antifibrotic drug nintedanib to treat lung ADC patients in combination with docetaxel [8,9].

In addition to their therapeutic relevance, studies *in vitro* have reported the prognostic value of epigenetic and transcriptional signatures associated with pulmonary TAFs [10,11]. In contrast, little is known on the clinical relevance of standard markers of activated fibroblasts in histologic samples from NSCLC patients. Thus very few studies have examined the prognostic value of stromal alpha-smooth muscle actin (α-SMA) in lung cancer, which is the gold standard marker of fibroblast activation [12]; moreover these studies have reported contradictory results [13,14], underscoring that the prognostic value of α-SMA in NSCLC remains unclear. In addition to α-SMA, the deposition of fibrillar (type I and III) collagens is another common marker of activated fibroblasts; however, to our knowledge their prognostic value in NSCLC has not been determined. To address this gap of knowledge we conducted a retrospective multicenter study of the prognostic value of standard markers of activated fibroblasts in using tissue microarrays (TMAs) containing samples from a cohort of early stage surgically-treated NSCLC patients gathered from multiple hospitals in Spain [15]. For this purpose we performed a quantitative image analysis of both α-SMA immunostaining and picrosirius red (PSR) staining of fibrillar collagens imaged with bright field and polarized microscopy, respectively, and combined these data with clinical information including survival gathered within a 3 year follow-up.

2. Materials and methods

2.1. Patients and tissue samples

This study involved the retrospective analysis of tissue samples from surgical patients collected by multiple Spanish hospitals belonging to the Bronchogenic Carcinoma Cooperative Group of the Spanish Society of Pneumology and Thoracic Surgery (GCCB-S) [15], as part of their contribution to the 8th edition of the IASLC staging project [16]. The initial cohort included 220 patients that were observed during a minimum of 3 years. Eighty-three patients died within the three years after surgery (39.7%). Histologic diagnosis and staging was conducted in accordance with the 8th edition of the IASLC staging project [17]. The initially gathered clinicopathologic variables are described elsewhere [18], and included smoking status, comorbidities, blood analyses, tumor location, staging, lung function, surgical treatment,

pathological diagnosis and PET imaging. Survival was assessed yearly. The experimental protocol was approved by the Ethics Committee of the study (Fundació Parc Taulí, PI12/02040) and by the Ethics Committees of all participating centers. Written informed consent was obtained from all patients.

2.2. Tissue microarray construction

Formalin-fixed paraffin embedded tissue samples were obtained from participating hospitals and stored at the CIBERES Pulmonary Biobank Platform (PBP). Three expert pathologists evaluated the samples, confirmed the histologic diagnosis and selected a representative tumor area for core extraction and subsequent Tissue Microarray (TMA) analysis. TMAs were prepared at the Morphology Core Facility at the Center for Applied Medical Research (CIMA) of the University of Navarra (Pamplona, Spain). TMAs were constructed using a manual tissue arrayer (MTA-1, Beecher Instruments). Three cylinders of 1 mm in diameter were obtained within a representative tumor region for each tumor sample, cut in 3 μm sections with a microtome (Microm, HM350S), and distributed as 3 sections per sample. Each TMA included samples from either ADC, SCC or other histologic subtypes, and were stored in paraffin until use.

2.3. Histology

Fibrillar collagens were stained with PSR, whereas α-SMA and Ki-67 were stained by immunohistochemistry. α-SMA and PSR stainings were conducted with the Bond automated system (Leica Microsystems) as described [19,20]. Nuclei were counterstained with hematoxylin. α-SMA, PSR and Ki-67 were visualized with bright field illumination with an upright microscope (BX43, Olympus) coupled to a digital camera (DP72, Olympus) using a 10× objective (Olympus). PSR staining was also imaged with an upright microscope (DMRB, Leica) equipped with polarized filters coupled to a digital camera (DFC450, Leica) using a 10×/0.25 NPlan objective (Leica). Vascular invasion (arterial or venous) was assessed by examining morphological infiltration of vein walls in H&E stainings.

2.4. Image analysis

All image processing was carried out with Image J [21] under the guidance of one of our pathologists (JR). Large void regions were manually removed to prevent overestimating the total area. For bright field images, each raw file was color deconvoluted —using either H-DAB (for α-SMA) or FastRed FastBlue DAB (for PSR)— and the suitable color channel was binarized and used to calculate the positive area fraction (%) over the total sample area (Suppl. Fig. S1). Area fraction was averaged for all images per patient (n = 3) to elicit the final patient percentage as α-SMA% or PSR-BF% (for PSR imaged with bright field). α-SMA images were also used to assess the percentage of necrotic area for each patient by manually outlining the necrotic regions and computing the corresponding area fraction. Similarly, images of PSR staining visualized with polarized light (PSR-PL) were converted into greyscale, inverted, binarized and used to compute the percentage (%) of positive area, which was averaged for each patient to elicit the final percentage as PSR-PL%. The number of positively stained nuclei for Ki-67 was counted and expressed as a percentage (Ki-67%) as described [20].

2.5. Statistical analysis

All statistical analyses were performed with the widely-used computing environment R-software, using computing functions of the base, survival, survivalROC and coin packages. Overall survival functions were assessed using the Kaplan-Meier estimator. Survival curves were compared by applying the Tarone-Ware test. Association between

quantitative variables was assessed by the Pearson's or Spearman correlation coefficient as required. Association between qualitative variables was evaluated by the chi-square test. When the applicability conditions were not met, Fisher's exact test was used. Comparisons of means were performed by Student's t-test. For each marker, optimum thresholds were computed by maximising the Youden's index J, which is defined as $J = $ Sensitivity + Specificity – 1 [22,23]. Adjusted hazard ratios were estimated by fitting the Cox's proportional hazards regression model as described in the main text. P-values were determined by likelihood ratio test and score test. Statistical significance was assumed at $p < 0.05$, whereas $p < 0.1$ was interpreted as marginally significant.

3. Results

3.1. Description of clinicopathologic data

We analyzed retrospectively TMAs containing samples from a cohort of 220 surgical patients gathered from multiple hospitals in Spain, which were observed during a minimum of 3 years. TMAs included samples from 3 representative tumor regions for each patient. The clinicopathologic features of our cohort and their overall survival (OS%) 3 years after surgery are shown in Table 1. The median patient age

Table 1
Cumulative OS% rates (36 months) of clinicopathologic variables.

Clinical variable	n (%)	OS (%)	p-value
Age (y.o.)			
< 65	90 (43.3%)	65.0	0.12
≥ 65	118 (56.7%)	56.3	
Gender			
Female	30 (14.4%)	70.0	0.38
Male	178 (85.6%)	58.3	
Race			
Caucasian	208 (100%)	60.3	n.a.
Other	0	n.a.	
Smoking history			
Never	20 (9.6%)	55.0	0.40
Former	101 (48.6%)	57.9	
Current	87 (41.8%)	63.7	
Weight loss			
absent (≤5 Kg)	190 (91.3%)	61.2	0.15
present (> 5 Kg)	18 (8.7%)	47.2	
Cardiovascular comorbidity			
No	118 (56.7%)	64.7	**0.066**
Yes	90 (43.3%)	54.0	
Histologic subtype			
Adenocarcinoma	105 (50.2%)	62.9	0.34
Squamous cell carcinoma	92 (44.0%)	55.6	
Large cell carcinoma	12 (5.7%)	74.1	
Differentiation grade			
Well/mod. differentiated (G1,G2)	151 (74.8%)	58.9	0.91
Poorly differentiated (G3)	51 (25.2%)	62.9	
Tumor stage (TNM)[a]			
IA1	6 (2.9%)	50.0	**< 0.001**[*]
IA2	21 (10.2%)	71.4	
IA3	31 (15.0%)	71.0	
IB	47 (22.8%)	82.4	
IIA	15 (7.3%)	60.0	
IIB	56 (27.2%)	55.7	
IIIA	29 (14.1%)	14.9	
IVA	1 (0.5%)	0.0	
Vascular invasion			
No (V0)	118 (69.8%)	60.4	0.23
Yes microscopic (V1)	49 (29.0%)	57.7	
Yes macroscopic (V2)	2 (1.2%)	0.0	

NOTE:
n.a.: not available.
Bold p-values indicate marginal significance ($p < 0.1$).
[*] $p < 0.05$ (log-rank test).
[a] According to 8th edition of the IASLC staging classification.

at the day of surgery was 66.2 years, with a range of 31.5–85.0 years, and the OS% was 60.3%. Most patients were male (85.6%) with a history of smoking as former (48.6%) or current (41.8%) smokers. Very few patients had a weight loss in the previous 6 months greater than 5 kg (8.7%); in contrast, nearly half (43.3%) had a cardiac comorbidity. The histological distribution was 50.2% ADC, 44.0% SCC and 5.7% large cell carcinoma (including both large cell carcinomas (2.4%) and large cell neuroendocrine carcinomas (3.3%)). Most patients exhibited a well or moderately well-differentiated histologic grade (74.8%), and their clinical TNM stage distribution declined with increasing stage (50.9% stage I, 34.5% stage II, 14.1% stage III and 0.5% stage IV). Histologic analysis revealed that vascular invasion was not observed in most patients (69.8%). As expected, the association between OS% (assessed 3 years after surgery here and thereafter) and the TNM stage was statistically significant ($p < 0.001$) [17]. In addition OS% was associated with cardiac comorbidity, although with marginal significance ($p = 0.07$).

3.2. Expression of fibroblast activation markers and their correlations

Even though collagen can be visualized with different histologic stainings, picrosirius red (PSR) has been pointed as the most specific for fibrillar collagens, for it enhances selectively the birefringence of collagen fibers, thereby rendering them visible with polarized microscopy [24,25]. Representative images of α-SMA and PSR stainings illustrating different coverage levels are shown in Fig. 1 and Suppl. Fig. S2. PSR revealed that stromal fibrillar collagens were often organized into thick layers surrounding groups of carcinoma cells. In agreement with the unique optical features of PSR, the fibrillar nature of collagen was more readily observable using polarized light than bright field illumination as shown in Fig. 1. Images of α-SMA staining revealed that it was localized in the cytoplasm and was largely restricted to stromal regions, as indicated by the visual overlap with PSR staining (Fig. 1 and Suppl. Fig. S2). Subsequent image processing enabled computing the percentage of positive area per image collected for each patient for either α-SMA (α-SMA%) or PSR imaged with bright field or polarized light — referred to as PSR-BF% and PSR-PL%, respectively— (Suppl. Fig. S1.). This image processing revealed that the positive area of PSR staining was generally larger with bright field than polarized light (Suppl. Fig. S1), which illustrates the known fact that linearly polarized light captures only a fraction of the total content of fibrillar collagens [24,25]. In addition, a strong positive correlation between PSR-BF% and PSR-PL% ($r = 0.79$, $p < 0.001$, Pearson's correlation coefficient) was observed, in agreement with previous observations [25]. Likewise we found a highly significant positive correlation between α-SMA% and either PSR-BF% ($r = 0.40$, $p < 0.001$) or PSR-PL% ($r = 0.26$, $p < 0.001$) (Suppl. Fig. S3), which is consistent with the common use of both α-SMA and fibrillar collagens as markers of activated fibroblasts.

3.3. Association of fibroblast activation markers with clinicopathologic variables

To analyze the association of α-SMA% and PSR% (which refers to both PSR-BF% and PSR-PL% here and thereafter) with clinicopathologic variables, we first identified a suitable threshold for each marker by maximising the Youden's index, which gives equal weight to both the marker's sensitivity and specificity [22,23]. This method is widely used in the diagnostic biomarker field, and is equivalent to the minimization of the sum of false negative and false positive rates, which is clinically appealing because it maximizes the overall correct diagnosis rate while minimizing the overall erroneous diagnosis rate [26]. This approach elicited two threshold candidates for α-SMA% and PSR-BF% that corresponded to two separate maximum in the Youden's index for these markers (i.e. 10.5% and 15.2% for α-SMA%, and 7.9% and 16.80% for PSR-BF%) and one threshold for PSR-PL% (3.29%) (Suppl. Fig. S4). The lower thresholds for α-SMA% and PSR-BF%
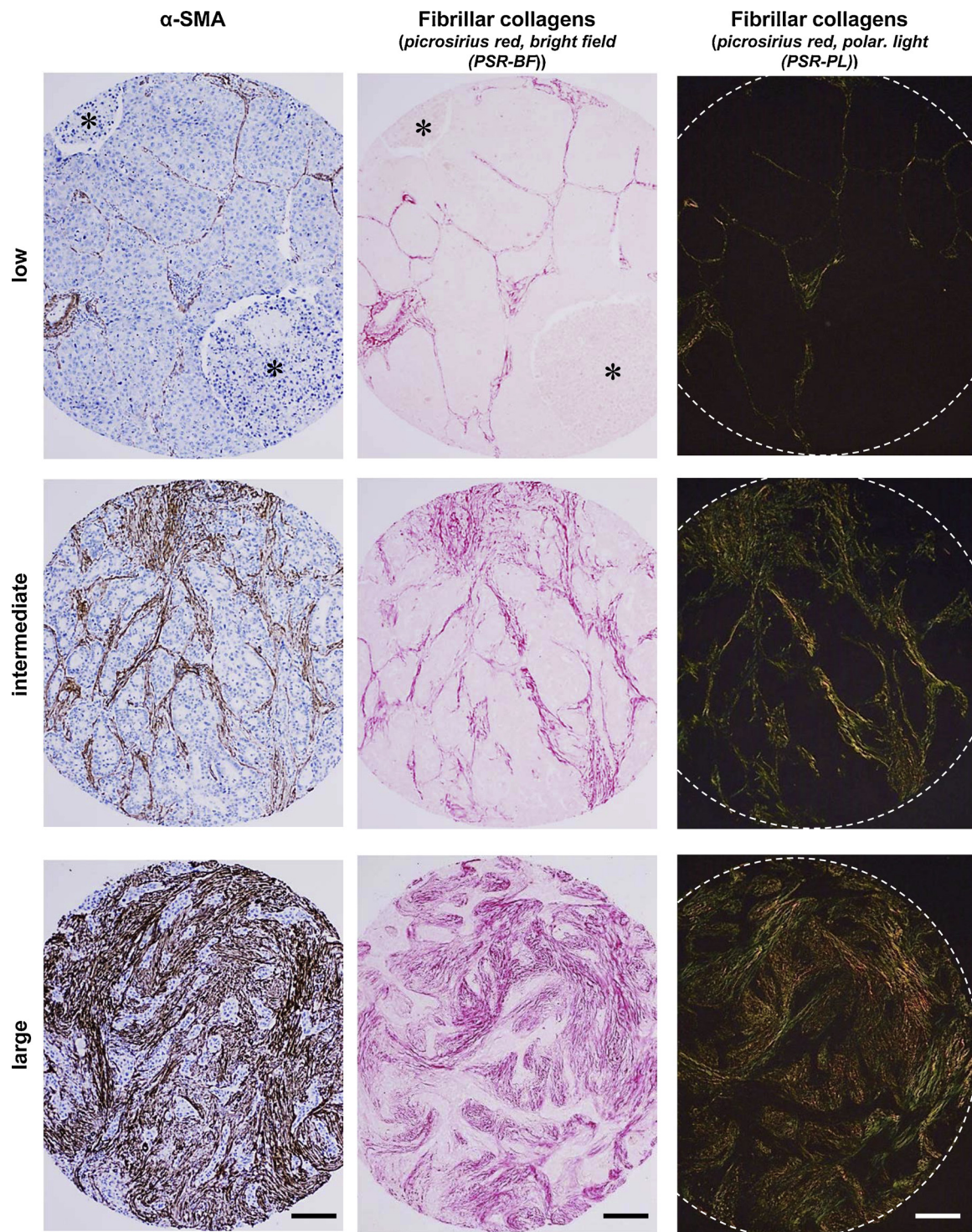
Fig. 1. Histologic images of standard fibroblast activation markers in NSCLC.
Representative images of histologic samples within TMAs of patients exhibiting either low, intermediate or large coverage of the stainings of TAF activation markers α-SMA and fibrillar collagens. The latter were stained with picrosirius red (PSR). α-SMA and PSR were imaged with bright-field microscopy (left and middle columns). PSR was further imaged with polarized microscopy (right column). Stars indicate necrotic areas used for subsequent analyses. Scale bars, 100 μm.

exhibited the highest sensitivity, whereas the corresponding higher thresholds exhibited the highest specificity (Suppl. Fig. S4). In agreement with previous work [27], we selected the lower thresholds (*i.e.* 10.5% for α-SMA%, 7.9% for PSR-BF% and 3.3% for PSR-PL%) for subsequent analyses, and used them in the main figures, whereas those analyses carried out with the alternative (higher) thresholds (*i.e.* 15.2% for α-SMA%, 16.8% for PSR-BF% and 3.3% for PSR-PL%) are shown in

Suppl. Fig. S5-S6 and Suppl. Tables S1-S2.

Clinicopathologic variables stratified by α-SMA%, PSR-BF% and PSR-PL% according to the latter thresholds are shown in Table 2. We found a significant association between PSR-BF% and both smoking history ($p = 0.01$) and histologic classification ($p < 0.001$). Furthermore, PSR-BF% was marginally associated with the maximum standardized uptake value (SUV$_{max}$) assessed by ^{18}F-fluorodeoxyglucose

Table 2
Association between TAF activation markers and clinicopathologic variables.

clinical variable	α-SMA% > 10.5%		PSR-BF% > 8%		PSR-PL% > 3.3%	
	Percentage	p-value	Percentage	p-value	Percentage	p-value
Age (y.o.)						
< 65	60.2%	0.65	74.7%	0.81	50.0%	0.64
≥ 65	64.5%		72.2%		54.3%	
Gender						
Female	62.1%	1.00	86.7%	0.12	63.3%	0.27
Male	62.7%		70.9%		50.6%	
Smoking history						
No (never)	57.9%	0.84	100.0%	**0.010**[*]	70.0%	0.16
Yes (former, current)	63.2%		70.3%		50.5%	
Weight loss						
absent (≤ 5 Kg)	62.9%	1.00	73.0%	1.0	51.3%	0.42
present (> 5 Kg)	60.0%		76.5%		64.7%	
Cardiovascular comorbidity						
No	66.4%	0.27	75.4%	0.53	53.0%	0.96
Yes	57.5%		70.5%		51.7%	
Histologic subtype						
Adenocarcinoma	60.0%	0.52	84.0%	**< 0.001**[*]	53.9%	0.75
Squamous cell carcinoma	65.6%		64.8%		49.5%	
Large cell carcinoma	n.a.		41.7%		58.3%	
Differentiation grade						
Well/mod. differentiated (G1,G2)	63.9%	0.65	75.3%	0.78	54.1%	0.41
Poorly differentiated (G3)	58.7%		72.0%		46.0%	
Tumor stage (TNM)						
IA1	40.0%	0.66	80.0%	0.99	80.0%	0.83
IA2	78.9%		76.2%		57.1%	
IA3	57.7%		77.4%		48.4%	
IB	63.6%		73.3%		47.8%	
IIA	66.7%		73.3%		60.0%	
IIB	56.6%		69.1%		49.1%	
IIIA	65.4%		74.1%		57.1%	
IVA	100.0%		100.0%		100.0%	
Vascular invasion						
No (V0)	67.3%	0.40	77.2%	0.39	59.6%	0.18
Yes (V1, V2)	58.7%		69.4%		47.1%	

Bold p-values indicate marginal significance (p < 0.1).
   * p < 0.05 (χ^2 test).

positron emission tomography, which is indicative of the regional glucose uptake in the primary tumor, yielding 11.0 ± 6.1 for PSR-BF% > 8% and 9.1 ± 5.9 for PSR-BF% ≤ 8% (p = 0.069). In contrast, no further associations were observed between other TAF activation markers and any other clinicopathologic variable. Thus, despite the significant correlations between all activation markers, only PSR-BF% was significantly associated with selected clinicopathologic data, thereby supporting that distinct TAF activation markers may be indicative of somewhat distinct features of the desmoplastic tumor stroma.

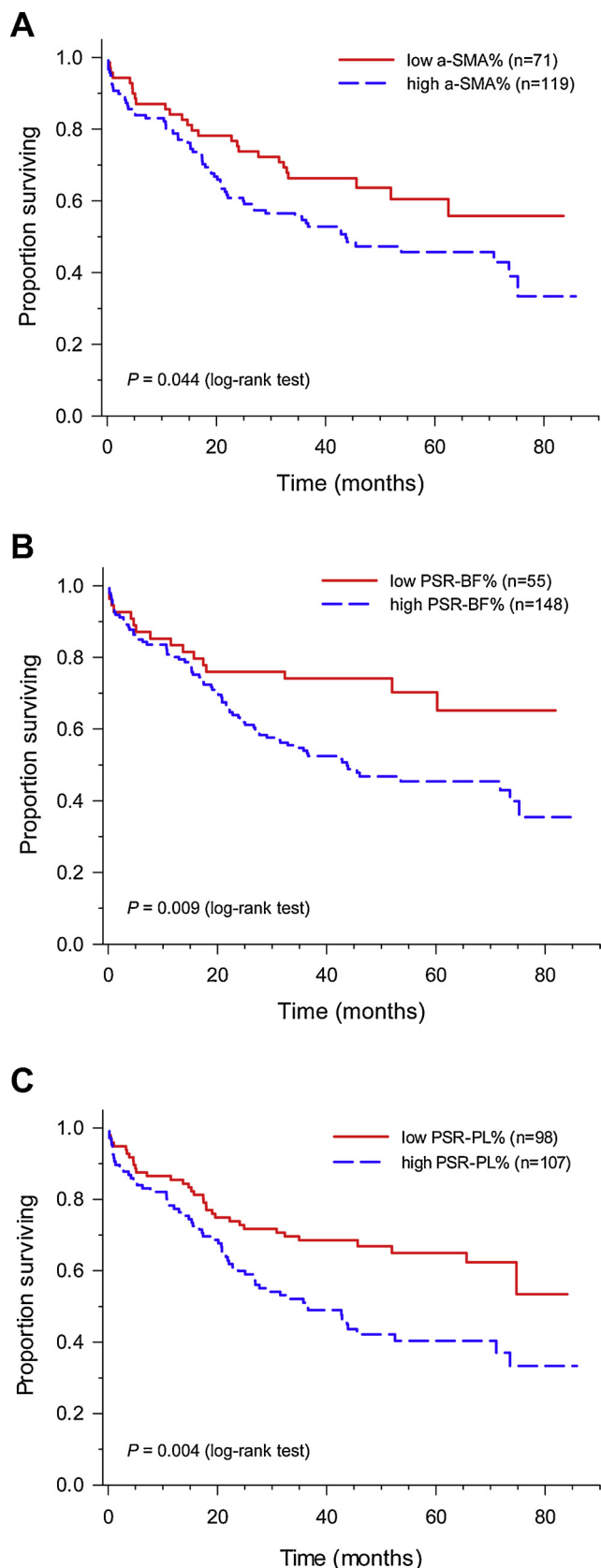### 3.4. Association of fibroblast activation markers with overall survival OS%

The thresholds described in the previous section were used as cut-offs to assess the Kaplan-Meier survival curves for each fibroblast activation marker. Remarkably, the group of patients with high levels of the activation markers (i.e. above the cut-off) consistently exhibited lower survival with statistical significance, including α-SMA% (p = 0.04, log-rank test), PSR-BF% (p = 0.009) and PSR-PL% (p = 0.004) (Fig. 2). These findings reveal that the histologic coverage of both α-SMA and fibrillar collagens within the desmoplastic stroma are associated with poor prognosis in NSCLC, and identify that PSR analyzed through polarized light microscopy is particularly useful in terms of predicting poor outcome.

To discern whether the prognostic value of TAF activation markers is already captured by the current gold standard of tumor staging based on TNM, we introduced either α-SMA%, PSR-BF% or PSR-PL% and tumor stage in a Cox regression model for multivariate OS% analysis.

Given the close relationship between OS% and cardiac comorbidity reported in Table 1, we also included the latter variable in the analysis. Of note, all TAF activation markers were independent prognostic factors, with the largest significance found in fibrillar collagens (PSR-BF%, p = 0.008 (likelihood ratio test); PSR-PL%, p = 0.004) compared to α-SMA% (p = 0.049). The results of the multivariate analysis are shown in Table 3, and revealed that patients with PSR-BF% above the cut-off (8%) had an adjusted 129% increased risk of death (HR = 2.29; 95% CI, 1.33–3.97; p = 0.004). Similarly, those patients with PSR-PL% larger than the cut-off (3.3%) had 94% increased risk of death (HR = 1.94; 95% CI, 1.26–2.99; p = 0.003), whereas patients with α-SMA% larger than the 10.5% cut-off had 89% increased risk of death (HR = 1.89; 95% CI, 1.17–3.04; p = 0.009). Cardiac comorbidity was also a significant independent prognostic factor for all markers, in agreement with previous reports [28]. These results reveal that the adjusted increased risk of death associated with the histologic coverage of either α-SMA or fibrillar collagens analyzed by PSR staining does not depend on a particular stage. In contrast, a multivariate analysis with an expanded list of clinicopathological variables (Age, Smoking history, Histologic subtype, and Vascular invasion) did not reveal additional independent prognostic factor consistently across the 3 stromal variables examined (Suppl. Table S3).

3.5. Association of fibrillar collagens with cancer-relevant pathophysiological processes

Once established the prognostic value of standard TAF activation markers in NSCLC, we began to examine potential underlying

Fig. 2. Survival analysis of NSCLC patients stratified according to standard fibroblast activation markers.
Kaplan-Meier survival curves stratifying patients according to α-SMA% (A), PSR-BF% (B) and PSR-PL% (C). For each marker, the low and high expression groups correspond to patients exhibiting a percentage of positive area below or equal/greater than the threshold, respectively.

pathophysiological processes. Our observed association between PSR-BF% and the regional glucose uptake (SUVT) prompted us to examine a potential association with proliferation by analyzing Ki-67 staining. In addition, we examined other tumor-promoting biological processes previously associated with increased fibrillar collagens, including invasion and hypoxia [5], by analyzing quantitatively vascular invasion and tumor necrosis, respectively, for necrosis is frequently used as a surrogate marker of hypoxia [29]. The information on vascular invasion was initially gathered in our clinicopathologic dataset, whereas both Ki-67 and necrosis were assessed as percentage of positive area by quantitative image analysis of α-SMA stainings as shown in Fig. 1, and were referred to as Ki-67% and necrosis%, respectively. Of note, all TAF activation markers consistently showed a significant positive association with necrosis% as indicated in Fig. 3 (α-SMA%, $p < 0.001$; PSR-BF%, $p = 0.02$; PSR-PL%, $p = 0.03$). In contrast no significant associations were found between Ki-67% or vascular invasion and any of the TAF activation markers. These results reveal a novel strong association between the extent of TAF activation, tumor necrosis and poor survival in surgical NSCLC patients.

Finally we examined to what extent the observations reported here were specific for the particular threshold selection that maximized the Youden´s index by re-analyzing the data using the alternative thresholds for α-SMA% (15.5%) and PSR-BF% (17%), which exhibit maximum specificity rather than sensitivity (Suppl. Fig. S4). In agreement with our initial findings, stratifying patients for each TAF marker according to the alternative thresholds elicited significant associations with both poor survival (Suppl. Table S2 and Suppl. Fig. S5) and necrosis (Suppl. Fig. S6), although the association between PSR-BF% and survival was marginally significant. Indeed, we only found minor differences in terms of fewer associations with clinicopathologic data (Suppl. Table S1) when using the alternative cut-offs, thereby reassuring that all thresholds obtained through the maximization of Youden´s index provided consistent results.

4. Discussion

A hallmark of NSCLC and other solid tumors is the presence of a stiff desmoplastic stroma rich in activated TAFs in the background of an excessive deposition of fibrillar collagens [5]. Stromal TAFs have been implicated in virtually all steps of tumor progression [7]. Therefore it is unsurprising that stromal proteins, including those related to TAFs, are receiving increasing interest as biomarkers or therapeutic targets [9,30]. However, the prognostic value of standard markers of activated TAFs had remained ill defined in NSCLC. Thus, the prognostic value of α-SMA had remained unclear due to conflicting observations [13,14], whereas that of fibrillar collagens has not been assessed directly.

Using a cohort of 220 NSCLC patients, we found that stromal α-SMA, assessed by quantitative image analysis, was significantly associated with shorter survival 3 years after surgery, and that this prognostic value was independent of TNM staging. In agreement with our findings, a histologic α-SMA scoring study conducted in China on a smaller cohort (n = 78) reported an association with adverse prognosis [14]. In contrast, a lack of association between α-SMA scoring and survival was reported in a study carried out in Norway with a larger cohort (n = 536) [13]. The reasons underlying the discrepancy of the Norwegian study compared to the Chinese study and ours are unclear. However it is conceivable that this discrepancy may be associated with the different methodologies used to analyze stromal α-SMA, since the Norwegian study used a single semi-quantitative scoring based on the percentage of positive stromal cells [13], whereas the Chinese study used the multiplication a percentage score and an intensity score [14]. In further agreement with our observations, positive correlations between higher stromal α-SMA and different markers of tumor progression have been reported in breast cancer [31] and gastric carcinoma [32]. In contrast, α-SMA expression was found not associated with survival in head and neck squamous cell carcinoma [33]. Collectively,

Table 3
Multivariate analysis for predictors of survival.

	α-SMA% > 10.5%		PSR-BF% > 8%		PSR-PL% > 3.3%	
	HR (95% CI)	*p*-value	HR (95% CI)	*p*-value	HR (95% CI)	*p*-value
TAF marker						
Low (ref.)[a]	1.00		1.00		1.00	
High	1.89 (1.18-3.04)	**0.009**[*]	2.29 (1.33-3.98)	**0.003**[*]	1.94 (1.26-2.99)	**0.003**[*]
Tumor stage						
IA1 (ref.)	1.00		1.00		1.00	
IA2	0.22 (0.06-0.90)	**0.035**[*]	0.40 (0.11-1.52)	0.18	0.46 (0.12-1.76)	0.26
IA3	0.20 (0.05-0.76)	**0.018**[*]	0.31 (0.08-1.13)	**0.076**	0.34 (0.09-1.23)	**0.10**
IB	0.17 (0.05-0.63)	**0.008**[*]	0.27 (0.08-0.98)	**0.047**[*]	0.29 (0.08-1.02)	**0.055**
IIA	0.41 (0.11-1.62)	0.21	0.64 (0.17-2.43)	0.51	0.66 (0.17-2.50)	0.54
IIB	0.51 (0.15-1.73)	0.28	0.81 (0.24-2.69)	0.73	0.88 (0.26-2.93)	0.83
IIIA	1.03 (0.30-3.58)	0.96	1.75 (0.52-5.95)	0.37	1.89 (0.56-6.42)	0.31
IVA	6.58 (0.63-68.97)	0.12	10.5 (1.02-108.22)	**0.048**[*]	10.28 (1.00-105.77)	**0.050**
Card. comor.						
No (ref.)	1.00		1.00		1.00	
Yes	1.86 (1.22-2.86)	**0.004**[*]	1.82 (1.20-2.75)	**0.005**[*]	1.76 (1.16-2.65)	**0.008**[*]

NOTE:

Bold *p*-values indicate marginal significance ($p < 0.1$).

[*] $p < 0.05$ (Cox hazard proportional model).

[a] < 10.5% for α-SMA%, < 8% for PSR-BF%, < 3.3% for PSR-PL%.

our data and previous observations support that stromal α-SMA is associated with poor outcome in NSCLC, and underline that a consensus method for α-SMA scoring is needed to confirm its prognostic value in other cancer types.

To our knowledge our study reports for the first time that the histologic coverage of stromal fibrillar collagens —assessed by image analysis of PSR staining with bright-field or polarized light— is a risk factor for increased death in resected NSCLC patients. Remarkably, the prognostic value of PSR was independent of TNM staging, indicating that PSR staining of fibrillar collagens is a novel independent prognostic biomarker in NSCLC. In support to our collagen analysis, a semi-quantitative scoring of tumor collagen content by van Gieson staining in a large cohort of NSCLC patients (n = 533) reported a trend between high collagen and decreased progression-free survival that attained marginal significance [30]. Likewise, indirect assessments of the collagen content in NSCLC patients from H&E stainings reported an association with poor survival in SCC (n = 220) [34] and ADC patients (n = 239) [35]. Altogether these observations indicate that the association between stromal collagen and adverse patient outcome is an emerging hallmark of NSCLC, and expand previous links between stromal collagen and increased risk of cancer [36,37]. More importantly, our results reveal that the assessment of the fibrillar collagen coverage in histologic samples by PSR staining may be a new clinical tool to identify those resected patients that are at higher risk of progression and death after surgery. Likewise, our data support that assessing the histologic coverage of fibrillar collagens may be a new suitable marker to help selecting which resected patients should be considered for adjuvant chemotherapy.

Stromal collagens can be stained with different methods, yet PSR has been pointed as the most sensitive owing to its unique ability to detect thin fibers [24,38]. PSR is also unique in that it changes the optical properties of fibrillar collagens by enhancing their birefringence, thereby allowing the direct visualization of fibers of type I and III collagens with polarized light [25]. However, it had remained unknown what visualization method of PSR (bright field or polarized light) could be more useful in terms of prognosis. Of note, our quantification of PSR imaged with polarized light (PSR-PL%) elicited the lowest *p*-values when analyzing survival data, thereby underlining that this imaging technique is particularly useful when using PSR as a prognostic biomarker. However, even though the specificity of PSR imaged with polarized light to detect fibrillar collagens has been extensively validated in organ fibrosis [38], the use of this method in

NSCLC and other cancer types is still rather limited [19,39]. On the other hand, PSR imaged with standard (non-polarized) bright-field (PSR-BF%) reported more associations with clinicopathological variables than PSR-PL%, in agreement with previous observations [25], thereby supporting that the combination of PSR visualization with both imaging methods provides complementary information.

The expression of genes coding for type I collagen has been consistently reported in transcriptional signatures associated with metastasis and shorter survival in lung ADC and other cancer types [40]. These observations strongly suggest that fibrillar collagens may play an active role in tumor progression in addition to being useful prognostic biomarkers. Indeed, defining tumor-promoting effects of fibrillar collagens is a matter of increasing research [5]. To begin to identify which of the latter effects might be more relevant in NSCLC, we sought for potential associations with three prevalent tumor-promoting biological processes: vascular invasion, proliferation and necrosis/hypoxia. The rationale for analyzing vascular invasion is based on previous studies using intravital imaging that showed how cancer cells migrate more rapidly in collagen-rich regions [41]. Likewise studies conducted in breast cancer revealed that high collagen amount, particularly when deposited radially from groups of carcinoma cells, promoted cancer cell migration [42]. In contrast, we did not find significant differences between histologic vascular invasion when stratifying patients according to their fibrillar collagen coverage. A possible interpretation of this negative result is that it is the spatial organization of the collagen fibers rather than their total amount, which is related to the histologic coverage as assessed in our study, what might be more relevant in terms of vascular invasion in NSCLC, as suggested elsewhere [42].

The rationale for examining proliferation was based on the increased proliferation and survival through β1 integrin/FAK signaling reported in TAFs and cancer cells cultured on hydrogels exhibiting tumor-like rigidities [19], which mimicked the matrix stiffening that arises from increased fibrillar collagen as reported *in vivo* and *in vitro* [39,43]. However, we did not observe a significant correlation between fibrillar collagens and the proliferation marker Ki-67. This negative result was somewhat unexpected, considering that we did find a marginal association between PSR-BF% and the regional glucose uptake marker SUVT, which is frequently used as a surrogate of cancer cell proliferation [44]. Yet it is worth considering that enhanced SUVT has been reported in fibrotic areas of idiopathic pulmonary fibrosis patients, which are rich in activated fibroblasts and fibrillar collagens but void of cancer cells [45]. Therefore it is conceivable that the larger
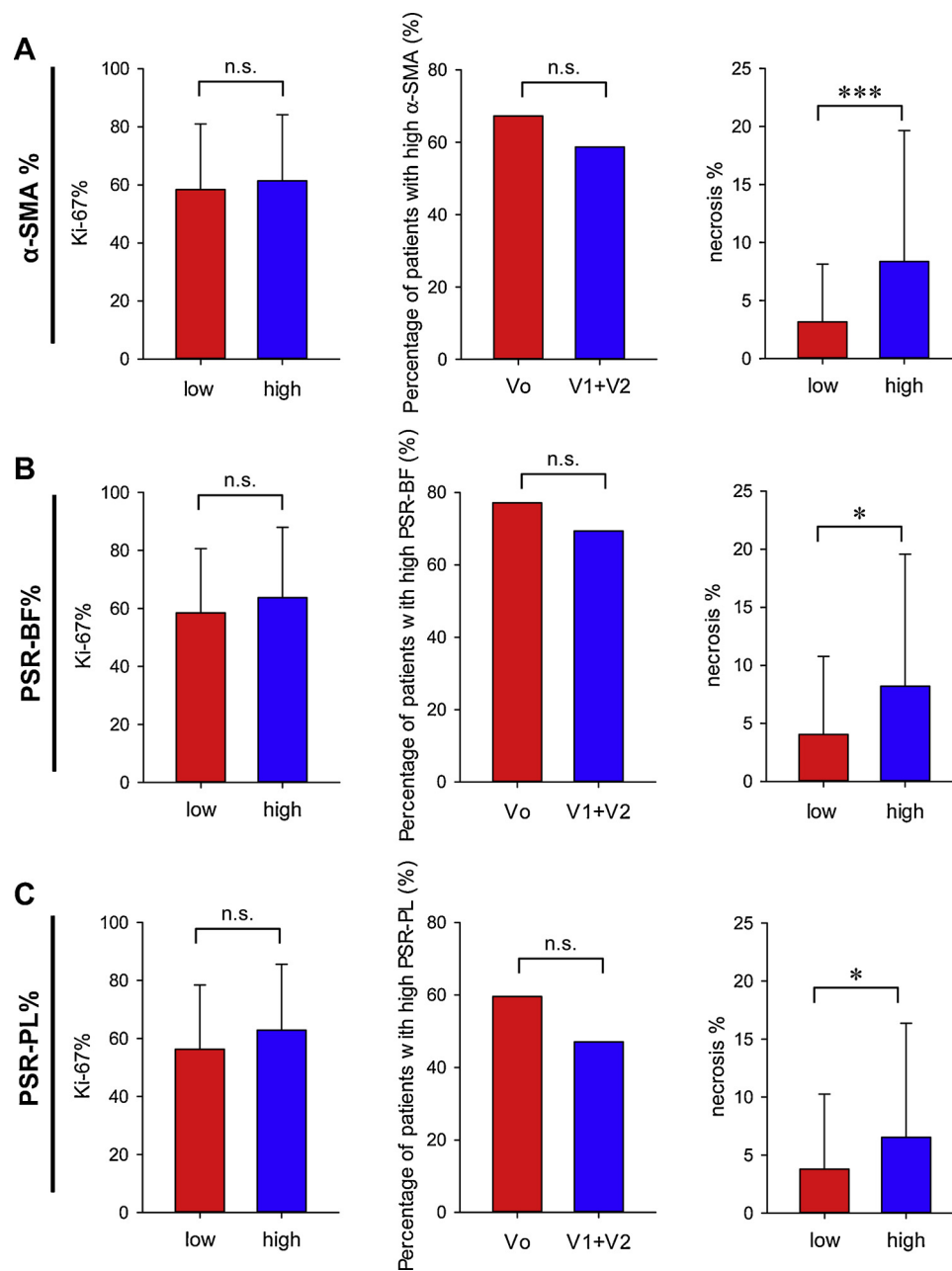
Fig. 3. Association of fibroblast activation markers with cancer-relevant biological processes.
Percentage of Ki-67 (marker of proliferation, left column), and necrosis (right column) for patients exhibiting activation markers below (low) or equal/greater (high) than the corresponding threshold for α-SMA% (A), PSR-BF% (B) and PSR-PL% (C). Middle column shows the percentage of patients with each TAF marker equal/greater than the corresponding cut-off according to their vascular invasion status. *, $p < 0.05$; **, $p < 0.01$; ***, $p < 0.005$.

SUVT observed here in patients with high PSR-BF% may partly reflect the increased metabolic demands of collagen biosynthesis rather than changes in cancer cell proliferation.

Unlike cancer cell proliferation and vascular invasion, we found a marked association between all TAF activation markers and necrosis. In agreement with our observation, tumour necrosis was reported to be an independent prognostic marker in NSCLC using a cohort of 178 surgically resected cases [46]. Future studies are required to further validate our observed association between stromal desmoplasia and tumor necrosis as well as to elucidate the potential causes and consequences of such association. However, it is worth noting that tumor necrosis is commonly used as indicative of hypoxia [29], and that the link between tumor hypoxia and aggressive phenotypes has been extensively documented [47]. Likewise, *in vivo* models of mammary tumors reported

that fibrotic tumors were also more hypoxic [48]. On the other hand, hypoxia enhances collagen expression *in vitro* [49], suggesting that the higher fibrillar collagen content found in samples with larger necrosis could be partly a direct consequence of hypoxia. In addition, increased fibrillar collagen has been also associated with collapsed microvessels and impaired drug delivery due interstitial pressure built up in solid tumors [50], thereby suggesting that a rise in stromal collagens could enhance hypoxia *per se*. In support of this interpretation, the antifibrotic drug nintedanib was shown to reduce the expression of fibrillar collagens in activated TAFs in *vitro* [9], and to provide a survival benefit in combination with the cytotoxic drug docetaxel in lung ADC [51]. Altogether, these previous observations suggest that the increased histologic coverage of fibrillar collagens could be both a cause and a consequence of necrosis/hypoxia, and support that antifibrotic drugs

aiming to downregulate collagen expression could help reducing also hypoxia in NSCLC.

5. Conclusions

In summary this study clarifies the prognostic value of α-SMA in NSCLC, and identifies the histologic coverage of fibrillar collagens assessed through PSR staining, particularly when imaged with polarized microscopy, as a novel and independent stromal biomarker associated with adverse prognosis in resected patients. Our analysis also identifies patients with large fibrillar collagen content to exhibit higher risk of recurrence and death, and reveal that they may benefit from a closer follow-up and should be considered for adjuvant chemotherapy. Our data also support a mechanistic relationship between collagen content and necrosis/hypoxia.

Declaration of competing interest

None.

Appendix A. Grupo Colaborativo en Cáncer de Pulmón CIBERES-CIBERONC-SEPAR-Plataforma Biobanco Pulmonar

Hospital Virgen del Rocío (Sevilla): Mª Ángeles González Castro, Ana Blanco, Rosa María Sánchez Gil. Hospital Mútua de Terrassa (Barcelona) and CIBERES (Madrid): Ramón Rami-Porta, Mireia Serra, Guadalupe González Pont. Hospital Son Espases (Palma de Mallorca), Institut d´investigació Sanitària de Palma (IdISPa) and CIBERES (Madrid): Jaume Sauleda and Sergio Scrimini. Hospital Germans Trias i Pujol (Barcelona) and CIBERES (Madrid): Esther Fernández, Pedro López de Castro, Carlos Martínez-Barenys, Jose Luis Mate. Fundación Jiménez Díaz-Universidad de Navarra (Madrid) and CIBERES (Madrid): Rosario Melchor, Mª Jesús Fernández-Aceñero, Luis Seijo. Hospital Joan XXIII (Tarragona): Leonardo de Esteban Júlvez, Ramon Magarolas. Hospital San Pedro de Alcántara (Cáceres): Julio Sanchez de Cos. Hospital Universitario Parc Taulí (Sabadell) and CIBERES (Madrid): Laura Millares, Eduard Monsó. Plataforma Biobanco Pulmonar CIBERES (Madrid): Cristina Villena. Centro de Investigación Médica Aplicada (CIMA), Universidad de Navarra, IDISNA (Navarra) and CIBERONC (Madrid): Maria Jose Pajares, Luis M. Montuenga. Universidad de Barcelona: Jordi Alcaraz. Hospital Clinic (Barcelona), Universidad de Barcelona, IDIBAPS and CIBERES (Madrid): Joan Albert Barberà. Universidad de Barcelona and IDIBAPS: Marta Cascante, Roldán Cortés, Cristina Balcells. IMIM Hospital del Mar (Barcelona) and CIBERES (Madrid): Esther Barreiro.

Appendix B. Supplementary data

Supplementary material related to this article can be found, in the online version, at doi:https://doi.org/10.1016/j.lungcan.2019.07.020.

References

[1] J.D. Minna, J.A. Roth, A.F. Gazdar, Focus on lung cancer, Cancer Cell 1 (1) (2002) 49–52.

[2] N. Howlader, A.M. Noone, M. Krapcho, D. Miller, K. Bishop, C.L. Kosary, M. Yu, J. Ruhl, Z. Tatalovich, A. Mariotto, D.R. Lewis, H.S. Chen, E.J. Feuer, K.A. Cronin, SEER Cancer Statistics Review, 1975–2014, National Cancer Institute, Bethesda, MD, 2017https://seer.cancer.gov/csr/1975_2014/.

[3] P. Boyle, C.J. Chapman, S. Holdenrieder, A. Murray, C. Robertson, W.C. Wood, P. Maddison, G. Healey, G.H. Fairley, A.C. Barnes, J.F.R. Robertson, Clinical validation of an autoantibody test for lung cancer, Ann. Oncol. 22 (2) (2011) 383–389.

[4] R.M. Bremnes, T. Donnem, S. Al-Saad, K. Al-Shibli, S. Andersen, R. Sirera, C. Camps, I. Marinez, L.T. Busund, The Role of Tumor Stroma in Cancer Progression and Prognosis Emphasis on Carcinoma-Associated Fibroblasts and Non-small Cell Lung Cancer, J. Thorac. Oncol. 6 (1) (2011) 209–217.

[5] M. Egeblad, M.G. Rasch, V.M. Weaver, Dynamic interplay between the collagen scaffold and tumor evolution, Curr. Opin. Cell Biol. 22 (5) (2010) 697–706.

[6] M. Gabasa, P. Duch, I. Jorba, A. Giménez, R. Lugo, I. Pavelescu, F. Rodríguez-Pascual, M. Molina-Molina, A. Xaubet, J. Pereda, J. Alcaraz, Epithelial contribution to the pro-fibrotic stiff microenvironment and myofibroblast population in lung fibrosis, Mol. Biol. Cell 28 (2017) 3741–3755.

[7] D. Ohlund, E. Elyada, D. Tuveson, Fibroblast heterogeneity in the cancer wound, J. Exp. Med. 211 (8) (2014) 1503–1523.

[8] F. Hilberg, G.J. Roth, M. Krssak, S. Kautschitsch, W. Sommergruber, U. Tontsch-Grunt, P. Garin-Chesa, G. Bader, A. Zoephel, J. Quant, A. Heckel, W.J. Rettig, BIBF 1120: triple angiokinase inhibitor with sustained receptor blockade and good antitumor efficacy, Cancer Res. 68 (12) (2008) 4774–4782.

[9] M. Gabasa, R. Ikemori, F. Hilberg, N. Reguart, J. Alcaraz, Nintedanib selectively inhibits the activation and tumor-promoting effects of fibroblasts from lung adenocarcinoma patients, Br. J. Cancer 117 (2017) 1128–1138.

[10] R. Navab, D. Strumpf, B. Bandarchi, C.Q. Zhu, M. Pintilie, V.R. Ramnarine, E. Ibrahimov, N. Radulovich, L. Leung, M. Barczyk, D. Panchal, C. To, J.J. Yun, S. Der, F.A. Shepherd, I. Jurisica, M.S. Tsao, Prognostic gene-expression signature of carcinoma-associated fibroblasts in non-small cell lung cancer, Proceedings of the National Academy of Sciences of the United States of America 108 (17) (2011) 7160–7165.

[11] M. Vizoso, M. Puig, F.J. Carmona, M. Maqueda, A. Velásquez, A. Gómez, A. Labernadie, R. Lugo, M. Gabasa, L.G. Rigat de Brugarolas, X. Trepat, J. Ramírez, N. Reguart, S. Morán, E. Vidal, A. Perera, M. Esteller, J. Alcaraz, Aberrant DNA methylation in non small cell lung Cancer associated fibroblasts, Carcinogenesis 36 (2015) 1453–1463.

[12] V. Mittal, T. El Rayes, N. Narula, T.E. McGraw, N.K. Altorki, M.H. Barcellos-Hoff, The microenvironment of lung cancer and therapeutic implications, in: A. Ahmad, S.M. Gadgeel (Eds.), Lung Cancer and Personalized Medicine: Novel Therapies and Clinical Management, 2016, pp. 75–110.

[13] T.K. Kilvaer, M.R. Khanehkenari, T. Hellevik, S. Al-Saad, E.-E. Paulsen, R.M. Bremnes, L.-T. Busund, T. Donnem, I.Z. Martinez, Cancer associated fibroblasts in stage I-IIIA NSCLC: prognostic impact and their correlations with tumor molecular markers, PLoS One 10 (8) (2015).

[14] Y. Chen, L. Zou, Y. Zhang, Y. Chen, P. Xing, W. Yang, F. Li, X. Ji, F. Liu, X. Lu, Transforming growth factor-beta 1 and alpha-smooth muscle actin in stromal fibroblasts are associated with a poor prognosis in patients with clinical stage I-IIIA nonsmall cell lung cancer after curative resection, Tumor Biol. 35 (7) (2014) 6707–6713.

[15] G.C.e.Cd.P.C.-C.-S.-P.B. Pulmonar, E. Monsó, L. Montuenga, J. Sánchez de Cos, C. Villena, Biological marker analysis as part of the CIBERES-RTIC Cancer-SEPAR strategic project on lung cancer, Arch. Bronconeumol. 51 (2015) 462–467.

[16] J. Sanchez de Cos Escuin, M. Serra Mitjans, J. Hernandez Hernandez, H. Hernandez Rodriguez, J. Abal Arca, I. Parente Lamelas, P. Leon Atance, A. Nunez Ares, L. Miravet Sorribes, A.I. Blanco Orozco, R. Melchor Iniguez, L. Garcia Aranguena, A. Arnau Obrer, R. Guijarro Jorge, J. Padilla Alarcon, J.C. Penalver Cuesta, M. Marinan Gorospe, E. Fernandez Araujo, G. Francisco Corral, S. Cerezo Gonzalez, G. Gonzalez Casaurran, S. Naranjo Gozalo, C. Alvarez de Arriba, M. Nunez Delgado, M.T. Gonzalez Budino, R. Magaroles, L. de Esteban Julvez, M.J. Pavon Fernandez, J.A. Gullon Blanco, B. de Olaiz Navarro, I. Escobar Campuzano, I. Macia Vidueira, S. Garcia Barajas, J. Herrero Collantes, J. Freixenet Gilabert, A. Saura Vinuesa, The spanish society of pulmonology and thoracic surgery lung Cancer cooperative Group-II registry. A descriptive study, Arch. Bronconeumol. 49 (11) (2013) 462–467.

[17] P. Goldstraw, K. Chansky, J. Crowley, R. Rami-Porta, H. Asamura, W.E.E. Eberhardt, A.G. Nicholson, P. Groome, A. Mitchell, V. Bolejack, S. Int Assoc Study Lung Canc, The IASLC lung Cancer Staging project: proposals for revision of the TNM stage groupings in the forthcoming (Eighth) edition of the TNM classification for lung Cancer, J. Thorac. Oncol. 11 (1) (2016) 39–51.

[18] R. Rami-Porta, V. Bolejack, D.J. Giroux, K. Chansky, J. Crowley, H. Asamura, P. Goldstraw, S. Int Assoc Study Lung Canc, M. Advisory Board, The IASLC lung Cancer Staging project: the new database to inform the eighth edition of the TNM classification of lung Cancer, J. Thorac. Oncol. 9 (11) (2014) 1618–1624.

[19] M. Puig, R. Lugo, M. Gabasa, A. Gimenez, A. Velasquez, R. Galgoczy, J. Ramirez, A. Gomez-Caro, O. Busnadiego, F. Rodriguez-Pascual, P. Gascon, N. Reguart, J. Alcaraz, Matrix stiffening and beta(1) integrin drive subtype-specific fibroblast accumulation in lung Cancer, Mol. Cancer Res. 13 (1) (2015) 161–173.

[20] M. Mateu-Jimenez, C. Fermoselle, F. Rojo, J. Mateu, R. Pena, A.J. Urtreger, M.J. Diament, E.D.Bd.K. Joffe, L. Pijuan, A.G. de Herreros, E. Barreiro, Pharmacological approaches in an experimental model of non-small cell lung

Cancer: effects on tumor biology, Curr. Pharm. Des. 22 (34) (2016) 5300–5310.

[21] M.D. Abramoff, P.J. Magelhaes, S.J. Ram, Image processing with ImageJ, Biophotonics Int. 11 (7) (2004) 36–42.

[22] E.F. Schisterman, N. Perkins, Confidence intervals for the Youden index and corresponding optimal cut-point, Communications in Statistics-Simulation and Computation 36 (3) (2007) 549–563.

[23] K. Skaltsa, L. Jover, J. Lluis Carrasco, Estimation of the diagnostic threshold accounting for decision costs and sampling uncertainty, Biom. J. 52 (5) (2010) 676–697.

[24] L. Rich, P. Whittaker, Collagen and picrosirius red staining: a polarized light assessment of fibrillar hue and spatial distribution, Brazilian Journal of Morphological Sciences 22 (2) (2005) 97–104.

[25] M.M. Diaz, M.D. Griffin, J.M. Slezak, E.J. Bergstralh, M.D. Stegall, J.A. Velosa, J.P. Grande, Correlation of quantitative digital image analysis with the glomerular filtration rate in chronic allograft nephropathy, Am. J. Transplant. 4 (2003) 248–256.

[26] K. Kaivanto, Maximization of the sum of sensitivity and specificity as a diagnostic cutpoint criterion, J. Clin. Epidemiol. 61 (5) (2008) 517–518.

[27] J.D. Cohen, L. Li, Y. Wang, C. Thoburn, B. Afsari, L. Danilova, C. Douville, A.A. Javed, F. Wong, A. Mattox, R.H. Hruban, C.L. Wolfgang, M.G. Goggins, M. Dal Molin, T.-L. Wang, R. Roden, A.P. Klein, J. Ptak, L. Dobbyn, J. Schaefer, N. Silliman, M. Popoli, J.T. Vogelstein, J.D. Browne, R.E. Schoen, R.E. Brand, J. Tie, P. Gibbs, H.-L. Wong, A.S. Mansfield, J. Jen, S.M. Hanash, M. Falconi, P.J. Allen, S. Zhou, C. Bettegowda, L.A. Diaz Jr, C. Tomasetti, K.W. Kinzler, B. Vogelstein, A.M. Lennon, N. Papadopoulos, Detection and localization of surgically resectable cancers with a multi-analyte blood test, Science 359 (6378) (2018) 926-+.

[28] J. Kravchenko, M. Berry, K. Arbeev, H.K. Lyerly, A. Yashin, I. Akushevich, Cardiovascular comorbidities and survival of lung cancer patients: medicare data based analysis, Lung Cancer 88 (1) (2015) 85–93.

[29] G.G. Van den Eynden, C.G. Colpaert, A. Couvelard, F. Pezzella, L.Y. Dirix, P.B. Vermeulen, E.A. Van Marck, T. Hasebe, A fibrotic focus is a prognostic factor and a surrogate marker for hypoxia and (lymph)angiogenesis in breast cancer: review of the literature and proposal on the criteria of evaluation, Histopathology 51 (4) (2007) 440–451.

[30] A. Soltermann, V. Tischler, S. Arbogast, J. Braun, N. Probst-Hensch, W. Weder, H. Moch, G. Kristiansen, Prognostic Significance of Epithelial-Mesenchymal and Mesenchymal-Epithelial Transition Protein Expression in Non-Small Cell Lung Cancer, Clin. Cancer Res. 14 (22) (2008) 7430–7437.

[31] M. Yamashita, T. Ogawa, X.H. Zhang, N. Hanamura, Y. Kashikura, M. Takamura, M. Yoneda, T. Shiraishi, Role of stromal myofibroblasts in invasive breast cancer: stromal expression of alpha-smooth muscle actin correlates with worse clinical outcome, Breast Cancer 19 (2) (2012) 170–176.

[32] Y. Fuyuhiro, M. Yashiro, S. Noda, S. Kashiwagi, J. Matsuoka, Y. Doi, Y. Kato, K. Muguruma, T. Sawada, K. Hirakawa, Myofibroblasts are associated with the progression of scirrhous gastric carcinoma, Exp. Ther. Med. 1 (4) (2010) 547–551.

[33] J. Valach, Z. Fik, H. Strnad, M. Chovanec, J. Plzak, Z. Cada, P. Szabo, J. Sachova, M. Hroudova, M. Urbanova, M. Steffl, J. Paces, J. Mazanek, C. Vlcek, J. Betka, H. Kaltner, S. Andre, H.J. Gabius, R. Kodet, K. Smetana, P. Gal, M. Kolar, Smooth muscle actin-expressing stromal fibroblasts in head and neck squamous cell carcinoma: increased expression of galectin-1 and induction of poor prognosis factors, Int. J. Cancer 131 (11) (2012) 2499–2508.

[34] Y. Takahashi, G. Ishii, T. Taira, S. Fujii, S. Yanagi, T. Hishida, J. Yoshida, M. Nishimura, H. Nomori, K. Nagai, A. Ochiai, Fibrous stroma is associated with poorer prognosis in lung squamous cell carcinoma patients, J. Thorac. Oncol. 6 (9) (2011) 1460–1467.

[35] A.M. Maeshima, T. Niki, A. Maeshima, T. Yamada, H. Kondo, Y. Matsuno, Modified scar grade — A prognostic indicator in small peripheral lung adenocarcinoma, Cancer 95 (12) (2002) 2546–2554.

[36] N.F. Boyd, L.J. Martin, M.J. Yaffe, S. Minkin, Mammographic density and breast cancer risk: current understanding and future prospects, Breast Cancer Res. 13 (6) (2011).

[37] H.B. El-Serag, Current concepts Hepatocellular Carcinoma, N. Engl. J. Med. 365 (12) (2011) 1118–1127.

[38] W. Malkusch, B. Rehn, J. Bruch, Advantages of sirius-red staining for quantitative morphometric collagen measurements in lungs, Exp. Lung Res. 21 (1) (1995) 67–77.

[39] I. Acerbi, L. Cassereau, I. Dean, Q. Shi, A. Au, C. Park, Y.Y. Chen, J. Liphardt, E.S. Hwang, V.M. Weaver, Human breast cancer invasion and aggression correlates with ECM stiffening and immune cell infiltration, Integr. Biol. 7 (10) (2015) 1120–1134.

[40] S. Ramaswamy, K.N. Ross, E.S. Lander, T.R. Golub, A molecular signature of metastasis in primary solid tumors, Nature Genet. 33 (1) (2003) 49–54.

[41] J. Condeelis, J.E. Segall, Intravital imaging of cell movement in tumours, Nat. Rev. Cancer 3 (12) (2003) 921–930.

[42] P.P. Provenzano, K.W. Eliceiri, J.M. Campbell, D.R. Inman, J.G. White, P.J. Keely, Collagen reorganization at the tumor-stromal interface facilitates local invasion, BMC Med. 4 (1) (2006) 38.

[43] J. Alcaraz, H. Mori, C.M. Ghajar, D. Brownfield, R. Galgoczy, M.J. Bissell, Collective epithelial cell invasion overcomes mechanical barriers of collagenous extracellular matrix by a narrow tube-like geometry and MMP14-dependent local softening, Integr. Biol. (Camb) 3 (12) (2011) 1153–1166.

[44] S.-m. Deng, W. Zhang, B. Zhang, Y.-y. Chen, J.-h. Li, Y.-w. Wu, Correlation between the Uptake of F-18-Fluorodeoxyglucose (F-18-FDG) and the Expression of Proliferation-Associated Antigen Ki-67 in Cancer Patients: A Meta-Analysis, PLoS One 10 (6) (2015).

[45] A. Justet, A. Laurent-Bellue, G. Thabut, A. Dieudonne, M.-P. Debray, R. Borie, M. Aubier, R. Lebtahi, B. Crestani, F-18 FDG PET/CT predicts progression-free survival in patients with idiopathic pulmonary fibrosis, Respir. Res. 18 (2017).

[46] D.E. Swinson, J.L. Jones, D. Richardson, G. Cox, J.G. Edwards, K.J. O'Byrne, Tumour necrosis is an independent prognostic marker in non-small cell lung cancer: correlation with biological variables, Lung Cancer 37 (3) (2002) 235–240.

[47] B. Muz, P. de la Puente, F. Azab, A.K. Azab, The role of hypoxia in cancer progression, angiogenesis, metastasis, and resistance to therapy, Hypoxia 3 (2015) 83–92.

[48] L.D. McPhail, S.P. Robinson, Intrinsic susceptibility MR imaging of chemically induced rat mammary tumors: relationship to histologic assessment of hypoxia and fibrosis, Radiology 254 (1) (2010) 110–118.

[49] V. Falanga, L. Zhou, T. Yufit, Low oxygen tension stimulates collagen synthesis and COL1A1 transcription through the action of TGF-beta 1, J. Cell. Physiol. 191 (1) (2002) 42–50.

[50] R.K. Jain, J.D. Martin, T. Stylianopoulos, The Role of Mechanical Forces in Tumor Growth and Therapy, M.L. Yarmush Annual Review of Biomedical Engineering, Vol. 162014, 321-346.

[51] M. Reck, R. Kaiser, A. Mellemgaard, J.-Y. Douillard, S. Orlov, M. Krzakowski, J. von Pawel, M. Gottfried, I. Bondarenko, M. Liao, C.-N. Gann, J. Barrueco, B. Gaschler-Markefski, S. Novello, L.U.-L.S. Grp, Docetaxel plus nintedanib versus docetaxel plus placebo in patients with previously treated non-small-cell lung cancer (LUME-Lung 1): a phase 3, double-blind, randomised controlled trial, Lancet Oncol. 15 (2) (2014) 143–155.